

Instrumental Measurements of Water and the Surrounding Space During a Randomized Blinded Controlled Trial of Focused Intention

[Luís Carlos Matos](#), MTCM,¹ [Sara Cristina Santos](#), MEng,¹ [Joel G. Anderson](#), PhD, CHTP,² [Jorge Machado](#), PhD,³ [Henry Johannes Greten](#), PhD,^{3,4} and [Fernando Jorge Monteiro](#), PhD¹

Abstract

The main goal of this work was the assessment of measurable interactions induced by focused intention, frequently used in biofield practices such as Healing Touch and *Reiki*. Water, as the main component of the human body, was chosen as a model. Intention experiments were performed over 4 different days at a scheduled interval, during which 286 trained biofield practitioners from several countries were instructed to meditate with the intention to change the molecular vibrational state of water samples selected by a blinded operator. The experimental protocol was randomized, blinded, and controlled; the measured variables included Raman spectra and the pH and electrical conductance of the water, as well as the magnetic field and UV-VIS (ultraviolet-visible) radiation near the experimental spot. Although a direct causal relationship cannot be established, some measurements of the water samples, as well as the magnetic field and radiation near the experimental spot, were responsive during the experimental period.

Keywords: intention, nonlocality, meditation, Raman spectroscopy, water vibrational spectra

Paradigms are determined by cultural differences and perceptions of reality, and often define the borderline between science and pseudoscience. Indeed, the history of science is full of challenging anomalies that, by defying the dominant paradigm, were ignored by the scientific mainstream until explained.^{1,2} Over the past several decades, researchers have been interested in the effects and potential mechanisms of certain energy-healing practices or biofield therapies such as *Qigong*, Healing Touch, and *Reiki*.^{3,4} As a result, practitioners of traditional medicine and so-called “energy healers” have been involved in a wide number of studies.⁵⁻¹⁵ Philosophically, each of these biofield therapies relies on a “vital force” as the main driving mechanism of health, pathogenesis, and healing. This philosophical approach is an ancient and shared concept understood, for example, as *Qi*, *Ki*, *Prana*, *Ankh*, and *Pneuma* in Chinese, Japanese, Hindu, Egyptian, and Greek cultures, respectively.¹⁶

Qigong, used in Chinese medicine as traditional vegetative biofeedback therapy, considers the existence of a differential external protective field known as *Wei Qi*, which acts on the physical, emotional, and spiritual levels.¹⁷ The hypothetical existence of such a complex and dynamic biologic field within and around the body, which is involved in homeostasis,^{18,19} could be partially based on the electromagnetic field theory,²⁰⁻³⁰ on acoustic and thermal related effects,^{5,9,31,32} and possibly other subtle energy fields, which, in some cases, seem to generate physical changes that are measurable with current technological methods.^{3,18,33,34} However, some practices appear to act in a manner described as nonlocal, thus acting at a distance, possibly compromising consciousness or even transpersonal realities, transcendental or spiritual experiences,^{18,35} defying mainstream scientific concepts.^{36,37} Nevertheless, the first approach while studying these phenomena is often the correlation with physical aspects such as light, electricity, heat, sound, and magnetism, and for that, researchers have been using a wide variety of instruments and methods, including magnetometers, voltmeters, photometers, gamma radiation counters, sound equipment, and gas discharge visualization, among others.^{5,9,27,28} Indeed, the use of proper and reliable instrumentation is a key factor to both document the phenomena and

potentially to calibrate biofield practitioners. This represents a challenge in research given that the involved mechanisms remain unknown and the ability to trigger these effects could be a natural skill or the result of continuous practice.

Within this field of study, intention, which could be defined as a directed thought to elicit a certain response,³⁸ seems to play an important role in the process.³⁹ Although the biophysics of intention are still under debate, research has shown that an intended thought appears to be able to generate physical effects over inanimate objects and living things, from unicellular organisms to human beings.^{37,38,40-43} The nonlocality feature of this phenomenon is often associated with the concept of entanglement^{37,42,44,45} and aspects of consciousness and quantum physics in which mental processes are referred to as a triggering element.^{42,46,47} In the case of distant healing, the healer who directs his/her thought or intent to the patient comprises a single system even while physically separated. Thus, the concept of entanglement is used to describe a connection between 2 elements that exist even though separated across space.⁴⁸

This phenomenon has obvious implications and requires not only clinical and preclinical studies in humans but also proper research with objective models exempt from expectation, belief, and psychosocial factors, such as models using animals, plants, biomolecules, tissue samples, and cell cultures.⁴⁹ Accordingly, water, as the main component of the human body, stands as an obvious choice not only to avoid the aforementioned interactions but also to generate hypotheses to explicate the subsequent effects and relationships within complex biological systems. Water has been used as a model in several studies with outcomes that suggest some of its properties, such as the cooling rate, the molecular bonding as reflected by changes in the infrared spectra, the vibrational state as measured by Raman spectroscopy, scattered laser light, and the pH level, may be affected by intention.^{30,38,40,43,50-53}

Given these arguments, the question of whether the mind may or may not influence matter is of relevance, especially within a dialogue of conflicting cultural, religious, and scientific concepts. Therefore, based on the available literature, we established a rigorous experimental

protocol and used several instrumental methods able to detect changes in the physical properties of water. The main goal of this work was the assessment of measurable interactions hypothetically induced by focused intention, frequently used in practices such as Healing Touch and *Reiki*.

Materials and Methods

Study Design

The experimental protocol, schematically represented in [Figure 1](#), used a randomized, blinded, and controlled design. Experiments were conducted over 4 consecutive days, from September 8 to 11, 2015, (experimental day 1 [ED1] to ED4). The source of the intentional meditation was 286 trained practitioners affiliated with 2 nonprofit organizations: Healing Touch International (dba Healing Beyond Borders) and the Portuguese Association of *Reiki*. Members of these organizations were invited to participate in the study via email. Potential participants used a Google form to provide limited information (email address, level of training, city, country) to maintain anonymity. None of the participants were aware of the experimental measures used to collect data.

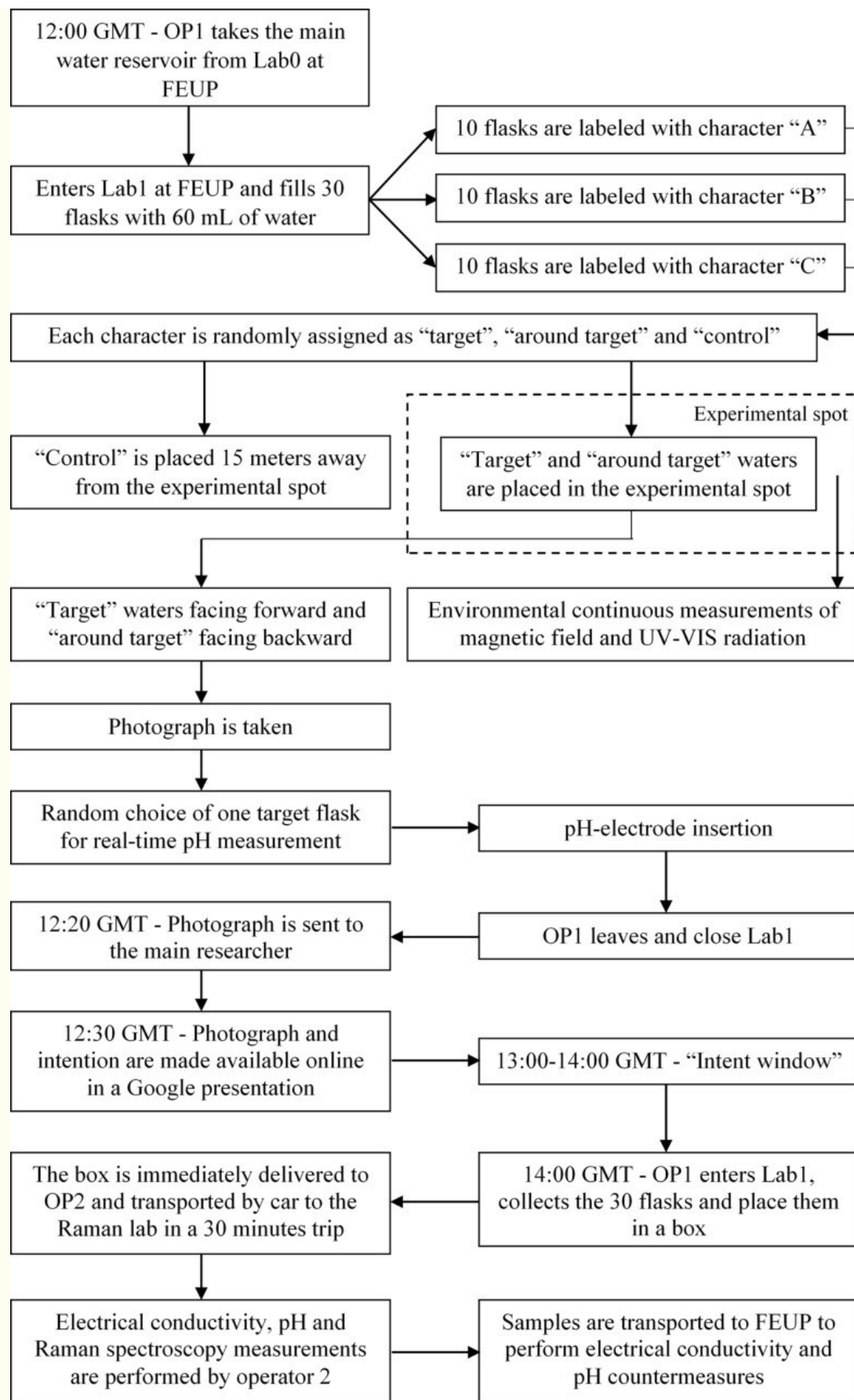


Figure 1.
Daily experimental protocol.

The sample of participants included 254 Healing Touch students, practitioners, and instructors with an average level of expertise of 7.2 years of practice (SD 7.1 years, median 5 years with a range of 0.25 to 40 years of practice) who were located in several countries according to the following distribution: the United States = 223; Canada = 24; Australia = 3; Peru = 3; and the Netherlands = 3. The 32 *Reiki* practitioners with an average level of expertise of 8.4 years of practice (SD 5.7 years, median 7 years with a range of 3 to 23 years of practice) were located in Portugal, from North to South of the country. Twelve of the *Reiki* practitioners held the level of *Shinpiden* (master or third level) and 20 the level of *Okuden* (second level), from the systems *Usui Reiki Ryoho*, Traditional Tibetan, and Essential.

Two independent experimental operators (operators 1 and 2), blinded to the study and without any knowledge of and connection to these biofield practices were instructed and trained to perform all required laboratory assessments systematically. An educational pilot plant laboratory (Lab1) located in the Department of Chemical Engineering of the Faculty of Engineering at the University of Porto was used during the experimental period. The laboratory was closed, kept in twilight without artificial light, and prohibited from any additional activity during the experiments. This laboratory was chosen because of the dimensions (7 m height, 7 m depth, 20 m length), which allowed for maintaining an average constant temperature of 24°C. Operator 1 (OP1) was the only person allowed to enter the laboratory to dispose of and collect the water samples after each experiment.

Commercial purified water was used and stored in a different laboratory in the same building. Each day, around 12:00 hours GMT, OP1 took the main water reservoir and entered Lab1 to fill the single-use 60 mL sterilized flasks (brand Deltalab). A total of 30 flasks were prepared: 10 of these were marked with the letter “A,” 10 with “B,” and 10 with “C.” Randomly, OP1 chose one of the characters as the control and placed the respective flasks 15 meters away from the experimental spot within the same laboratory. The other 20 flasks were randomly arranged on the experimental spot, and again, OP1 chose one of the characters to face forward (corresponding to the flasks with the target samples) and the other to face backward (corresponding to the flasks around the target); the random choice of

characters is shown in [Table 1](#). Flasks placed around the target samples were used to verify whether the intention was selective. All experimental design conditions were kept constant as the laboratory bench was marked with specific locations for the flasks and the measurement instrumentation. A photograph of the 20 experimental flasks was taken and a pH electrode connected to a data acquisition system, which saved data with a frequency of 1 data point every 5 seconds, was vertically inserted into one of the flasks with the character facing forward. A magnetic field sensor and a spectrometer were installed near the experimental spot and configured for continuous acquisition of the magnetic field strength and radiation in the range of 175 to 954 nm. Following this procedure, OP1 exited and closed Lab1, and around 12:20 hours GMT sent the photograph of the flasks with the target identified to the main researcher.

Table 1.

OP1 Random Choice of Characters.

Experimental Day	Target	Around Target	Control
ED1	A	B	C
ED2	C	A	B
ED3	B	C	A
ED4	A	C	B

Abbreviations: OP, operator; ED, experimental day.

The photograph was published using a Google document that was made available online at 12:30 hours GMT on the day of the experiment; a link to the document was emailed to all 286 practitioners enrolled in this study. Below the photograph, a defined intention was included:

To change the vibrational state of the water molecules contained in the flasks marked with the character...placed in the lab..., FEUP, Portugal.

The concept described (ie, “to change the vibrational state of the water molecules”) was understood among the practitioners as the action of “energizing the water,” for example, by allowing the imagination of molecular movement or structure dynamics. Although

the identification of the target was available at 12:30 hours GMT, the practitioners were instructed to meditate during a defined “intention window” set between 13:00 and 14:00 hours GMT. Each of the Healing Touch participants meditated for 10 minutes per day during the intention window, while the *Reiki* practitioners were free to meditate for the time they felt reasonable. To find the average meditation time, *Reiki* practitioners were instructed to register the time spent in meditation; a mean meditation time of 15 minutes was achieved, with a minimum of 2 minutes and a maximum of 45 minutes.

At 14:00 hours GMT, OP1 entered Lab1 to collect the flasks with the water and placed these in a box that was immediately delivered to operator 2 (OP2). OP2 transported the water samples by car between the Faculty of Engineering (FEUP) and the Raman laboratory located at the Institute of Material Physics in the Department of Physics and Astronomy of the Faculty of Sciences (approximately a 30-minute drive). OP2 performed Raman spectroscopy, pH, and electrical conductance measurements. The following day, the samples were transported back to FEUP to perform pH and electrical conductance countermeasures. The described protocol was repeated each day of the experimental period, and the collected data were delivered to the main researcher at the end of the study.

In addition to the measurements made from September 8 to 11, 2015, magnetic field strength and radiation, as well as real-time pH measurements, were taken on control days. On those days the laboratory conditions, the experimental spot arrangement, procedures, and timings were kept the same, differing only in the absence of intention between 13:00 and 14:00 hours GMT.

Instrumentation and Data Collection

Variables such as magnetic field strength, ultraviolet and visible radiation (UV-VIS wavelength range—175 to 954 nm), and real-time pH of the target water samples were measured by equipment set to continuous acquisition during the experimental period each day. Magnetic field strength was measured in the 0.32 mT range with a

resolution of 0.0002 mT with a Vernier Magnetic Field Sensor using a Hall-effect transducer connected to a Vernier LabPro interface. Data were collected using the Logger Pro 3.8.4 software. A ScanSpec UV-VIS spectrometer from Sarspec, equipped with a Sony ILX511 linear charge-coupled device (CCD) array 2048 pixels and with an entrance aperture of 50 μm , was used to measure the radiation spectra between 175 and 954 nm. Real-time pH was measured using a JUMO ecoLine glass pH electrode, with a ceramic diaphragm in the glass shaft, connected to a Hanna Instruments 209 pH meter equipped with a proportional DC analog output. The signal was collected by a NI DAQ card USB-6008 with 12-bit resolution and analyzed with a virtual interface programed in LabVIEW 8.2 from National Instruments.

Momentary measurements of pH and electrical conductance were performed for each sample with a HI8424 pH meter from Hanna Instruments equipped with a HI1230 electrode and with a GLP31 Conductimeter from Crison equipped with a 5293 conductivity cell. Countermeasures were performed with a Hanna Instruments 209 pH meter coupled to a glass membrane electrode and with a RE 388 TX conductimeter from EDT Instruments equipped with a glass dip cell. The equipment used for countermeasures was checked daily for calibration using standard buffers.

Unpolarized Raman spectra were obtained at room temperature, with a spectral slit width better than 1.5 cm^{-1} in the 1300 to 3900 cm^{-1} spectral range. The excitation was ensured by a 514 nm line of an argon laser with a power of 1.6 W. The conditions were kept constant for all scattering measurements. The scattered light was analyzed by a [T64000](#) Jobin-Yvon triple spectrometer operating in triple subtractive mode and equipped with a liquid nitrogen cooled CCD. Data were collected and analyzed using LabSpec5 software.

Statistical Analysis

Pearson's correlation analyses and t tests for independent samples were performed with Statistica for Windows release 7.0 to detect the

relationships between variables and to evaluate the statistical significance of the observed differences.

Results and Discussion

Changes in the magnetic field strength and radiation measured near the experimental spot were detected and found to coincide with the activities during the experimental period. The magnetic field strength profiles for each experimental day, as well the day before the beginning of the study, are shown in [Figure 2](#). Mean values per day, from 7 to 28 September, were calculated and are plotted in [Figure 3](#).

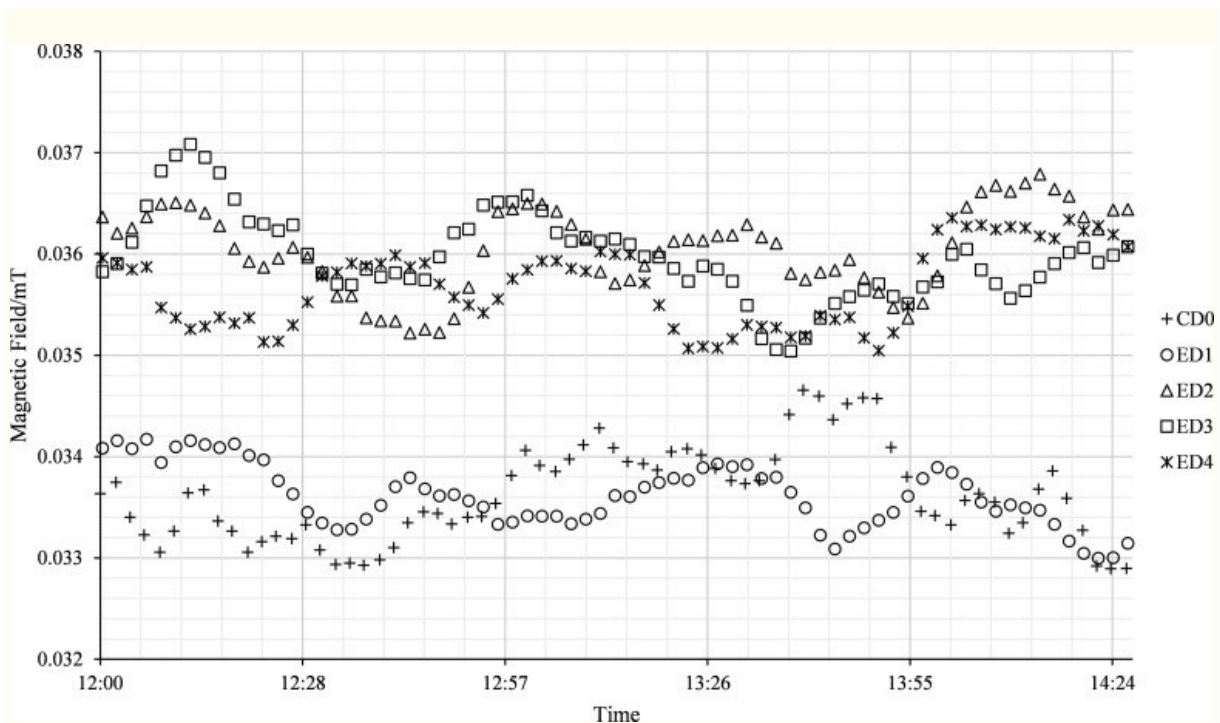


[Figure 2.](#)

Magnetic field strength near the experimental spot during the experimental week.

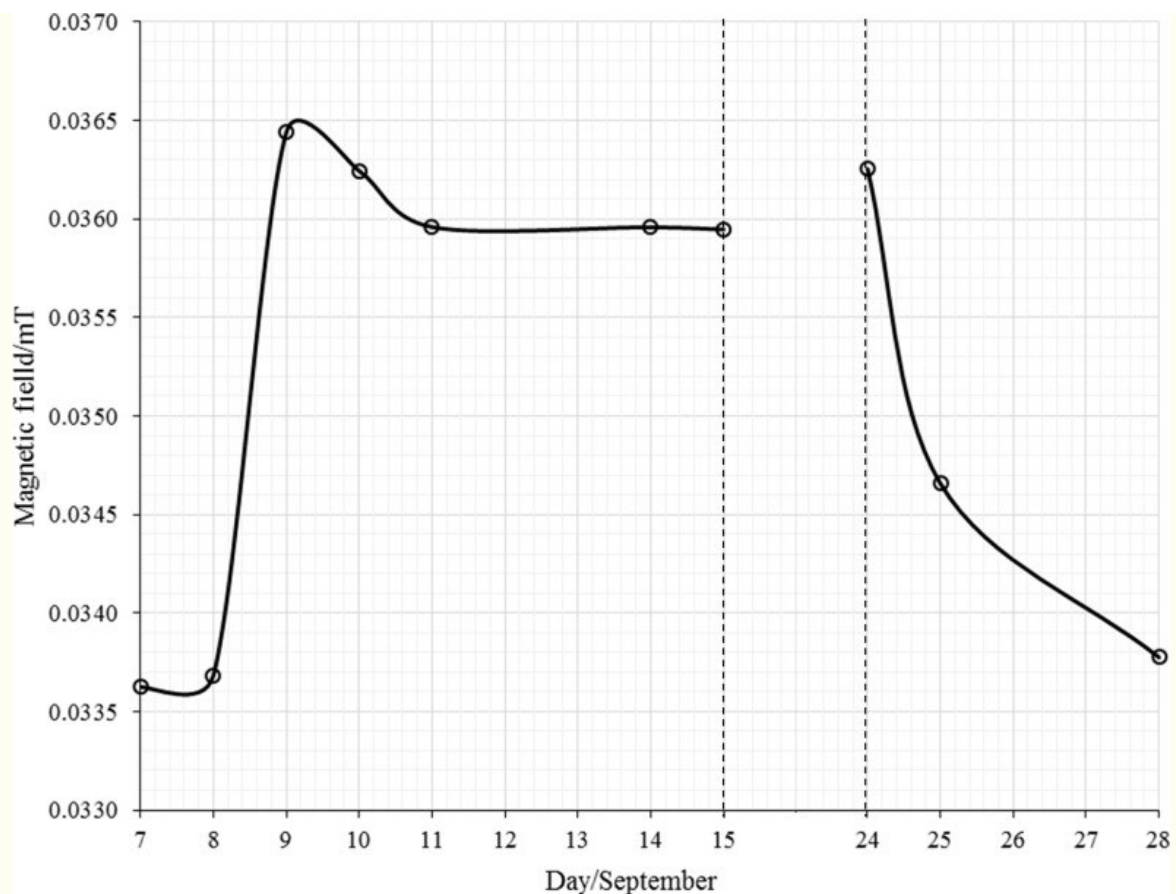


[Figure 3.](#)

Mean magnetic field strength recorded from 7 to 28 September.

An increase in the magnetic field strength was observed immediately after the first day. Specifically, on 7 September (CD0), the day before the first experimental day, the mean value was 0.0336 ± 0.0004 mT; the value increased to a maximum of 0.03644 ± 0.0005 mT on 9 September, followed by a slight decrease and remained constant until 15 September. The second part of this study was conducted under specific conditions between 15 and 24 September (data not shown). This gap of time and data are represented by the intermittent vertical lines in [Figure 3](#). From 24 September, the magnetic field strength decreased to 0.0338 ± 0.0003 mT. With the beginning of educational activities in the laboratory, the experimental conditions were compromised and no further measurements were possible. Nonetheless, from 30 October to 6 November, during a period of inactivity, we performed new measurements and found a mean magnetic field strength of 0.0339 ± 0.0005 mT, similar to the values obtained at the beginning of the study.

During the experimental activities, none of the 286 practitioners were in the vicinity of the laboratory. Additionally, none of them knew that magnetic field strength would be one of the studied variables. Because the magnetometer and probe were kept in the same position during all experiments and no inductive equipment was working nearby, we cannot point to a clear explanation for these kind of changes and correlations.

According to William A. Tiller, Professor Emeritus from the Department of Material Sciences and Engineering at the University of Stanford, a laboratory space can become changed or “conditioned” when submitted to a continuous intentional stimulus. Tiller and his colleagues claim that the fundamental symmetry state of the space can be altered by activating the indwelling-consciousness of that space to a higher level of physical reality, thus changing the electromagnetic gauge symmetry state of the experimental space, which in turn allows human intention to change the properties of materials significantly.^{[45,50,54–58](#)} Obviously this explanation is based on a paradigm-challenging model. In the present experiment, we observed a change in the magnetic field strength that followed a pattern and points to a hypothetical conditioning of the laboratory; however, we do not have causal data to support this argument.

To collect the maximum information possible, a spectrometer was used to measure the spectra between 175 and 954 nm. This piece of equipment was located 10 cm away and pointing toward the experimental spot where the target water samples were placed. The spectra were collected between 11:00 and 16:00 hours GMT with a frequency of 1 spectrum every 2 minutes. To evaluate any spectral changes during the experiments, 2 critical moments were considered: between 12:25 and 12:35 hours GMT when the photographs of the waters samples were available online, and between 12:55 and 13:05 hours GMT when the “intention window” began. Measurements were taken both during control and experimental days, and the mean values and dispersion of each critical moment were calculated ([Table 2](#)).

Table 2.

Intensity Mean Values and Dispersion Data of the UV-VIS Spectrum in the First and Second Critical Moments.

Wavele ngth Interval		ED1		ED2		ED3		ED4		CD1		CD2	
		Fir st	Seco nd	Fir st	Seco nd	Fir st	Seco nd	Fir st	Seco nd	Fir st	Seco nd	Fir st	Seco nd
175-375 nm	MI	3.3	2.4	2.4	3.2	2.8	2.8	2.2	4.2	2.7	2.7	3.0	2.9
	MD	2.4	2.0	1.6	1.8	1.8	2.3	1.5	2.4	1.6	1.4	1.8	1.9
	Ma xD	3.4	3.7	2.7	3.1	3.0	3.3	2.2	3.4	2.4	2.3	3.0	2.7
	Min D	1.6	1.2	0.6	0.8	1.1	1.6	0.6	0.9	0.9	0.5	1.1	0.9
375-575 nm	MI	16. 5	15.8	13. 0	11.0	14. 8	11.0	14. 9	16.3	15. 6	15.5	13. 9	14.5
	MD	2.7	8.2	2.2	4.6	3.1	6.3	3.3	6.8	1.8	2.6	2.7	2.6
	Ma xD	3.8	11.3	3.8	6.9	4.7	8.7	4.8	9.5	2.7	3.5	3.8	3.3
	Min D	1.7	3.7	0.9	2.1	1.9	3.4	2.1	2.6	0.9	1.4	1.8	1.8
575-775 nm	MI	4.8	4.6	7.6	5.0	4.4	4.6	4.2	6.5	5.3	4.6	5.3	3.4
	MD	4.0	3.7	3.3	4.7	2.4	4.3	2.5	2.8	2.4	2.9	3.2	2.9
	Ma xD	5.3	5.5	4.1	5.4	5.2	5.6	3.9	5.5	3.5	4.4	4.4	4.6
	Min D	1.6	2.8	2.3	3.1	1.1	2.3	1.6	0.9	1.5	1.8	1.9	1.6
775-954 nm	MI	2.0	0.6	1.6	2.3	0.0	2.3	1.5	3.1	1.1	0.6	3.2	1.4
	MD	4.4	3.4	2.5	4.7	3.6	3.0	3.8	3.2	2.5	2.8	3.0	3.2
	Ma xD	6.6	5.2	7.3	6.4	8.4	4.5	7.2	5.2	4.9	4.4	4.4	4.7
	Min D	3.2	2.3	1.3	3.1	1.6	2.1	1.9	1.9	1.1	1.2	1.8	1.6

Abbreviations: UV-VIS, ultraviolet-visible; ED, experimental day; CD, control day; MI, mean intensity; MD, mean dispersion; MaxD, maximum dispersion; MinD, minimum dispersion.

[Figure 4](#) shows the mean spectra and dispersion of 2 control days (CD1 and CD2) and 2 experimental days (ED1 and ED4). This analysis

allowed for the evaluation of the light-scattering properties around the experimental spot. We found a higher frequency of spectral changes with an increase in intensity during both critical moments on the experimental days. Specifically, this variability was more expressive during the critical moment set between 12:55 and 13:05 hours GMT, when the “intention window” began and during which all practitioners were instructed to meditate with the established intention.

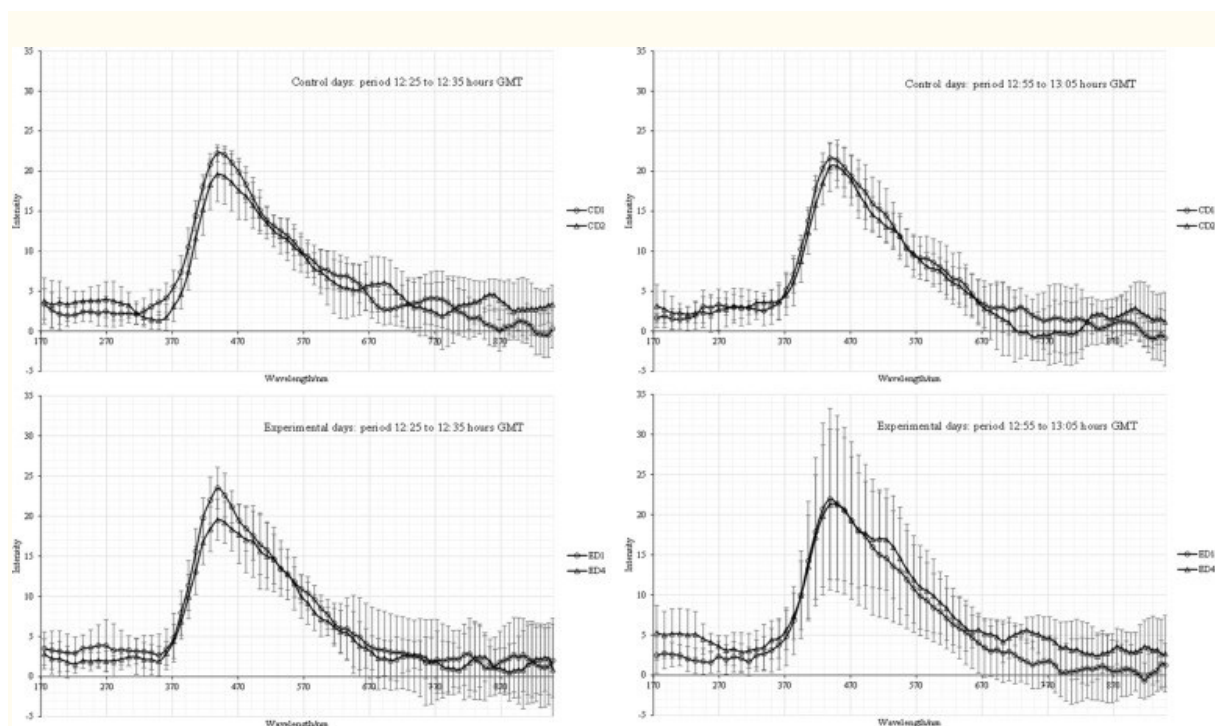


[Figure 4.](#)

Ultraviolet and visible spectrums of the environmental near the experimental spot.

This behavior is easily observed in the wavelength interval 375 to 575 nm during the second critical moment by comparing the mean and maximum dispersion values between both experimental and control days. Again, because the experimental conditions were kept constant, we do not have a plausible explanation for the changes outside of a hypothetical interference of the equipment or a specific higher instability of the overall light-scattering effects located around the experimental spot.

The sensitivity of pH to intention has been reported by other authors.[45,50,54-57](#) We used a real-time data acquisition system that was tested for sensitivity and stability during long periods and, therefore,

able to detect any eventual changes during the course of the experiments. We found that the instability mentioned above and the relationship with both critical moments was also noticed using real-time pH measurements. [Figure 5](#) shows the pH profiles on 3 experimental days (ED1—data not shown). On ED2, the pH remained stable until 13:00 GMT; from this point on, we noticed an increase followed by shifts in the tendency, reaching a higher value around 14:00 GMT. Similar results were observed on the other days. After 12:30 GMT, we detected a slight variability in all profiles that was evident on ED4. It should be mentioned that all the involved practitioners were instructed to meditate during the “intention window,” as this was set as a premise during the enrollment process. Nevertheless, because the practitioners were able to see the target at 12:30 GMT, we cannot guarantee that some may have started the intention earlier.

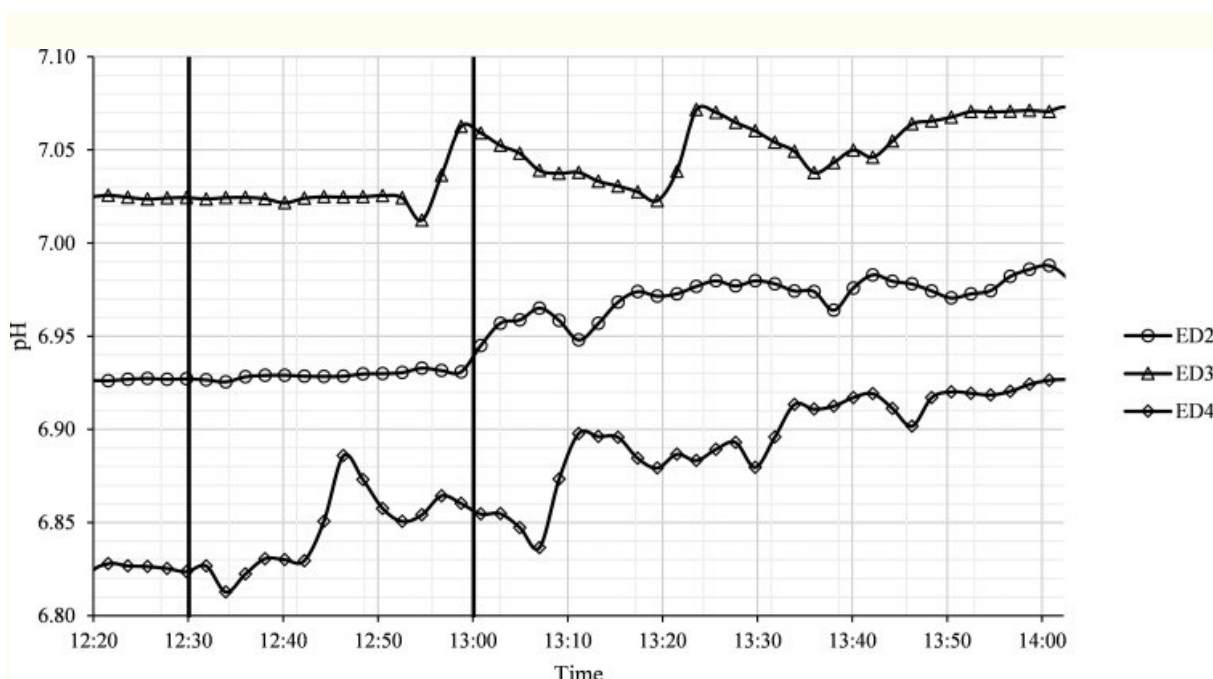


[Figure 5.](#)

Real-time pH of the targeted water during the experiments.

Both pH and electrical conductance measurements were performed before Raman spectroscopy. The measurements were made under adequate stirring conditions and automatic temperature compensation. Under normal conditions, a stable pH value should be obtained when the equilibrium electrochemical potential is achieved by the electrolyte-electrode system. In our work, OP2 reported

difficulties during pH measurements, with statements such as: “I didn’t understand why but in some samples the pH shoots to high values and then decreased....I thought that the pH meter had a malfunction”. In fact, this is visible in [Table 3](#), regarding the pH mean values and dispersion of the target water samples. Target water samples presented higher pH values and higher variability during these measurements, suggesting a higher sensitivity of the electrode in those samples. Although we cannot point to any reasonable explanation for these differential changes, some authors suggest that such an increase in pH could be related to a higher level of thermodynamic free energy.⁵⁹

Table 3.

pH and Electrical Conductance (mS cm⁻¹) of the Water at 25°C (Blinded Measurements and Countermeasures).

	ED1		ED2		ED3		ED4	
	pH	Conductivity	pH	Conductivity	pH	Conductivity	pH	Conductivity
A ^a	7.27		7.09		7.12		7.20	
	±	27.65 ± 0.13	±	27.11 ± 0.54	±	27.59 ± 0.13	±	27.44 ± 0.30
	0.12		0.07		0.02		0.08	
A ^b	7.26		7.11		7.08		7.15	
	±	26.85 ± 0.24	±	27.36 ± 0.26	±	27.57 ± 0.53	±	28.16 ± 0.55
	0.03		0.04		0.02		0.06	
B ^a	7.03		7.03		7.17		6.98	
	±	27.54 ± 0.11	±	27.23 ± 0.53	±	27.56 ± 0.18	±	27.14 ± 0.42
	0.17		0.05		0.08		0.08	
B ^b	7.00		7.07		7.14		7.06	
	±	26.74 ± 0.15	±	27.45 ± 0.55	±	27.99 ± 0.50	±	27.83 ± 0.43
	0.02		0.02		0.07		0.02	
C ^a	6.90		7.03		7.10		7.11	
	±	27.50 ± 0.10	±	27.51 ± 0.27	±	27.47 ± 0.33	±	27.36 ± 0.34
	0.11		0.14		0.08		0.08	
C ^b	6.90		7.15		7.12		7.14	
	±	26.64 ± 0.21	±	28.42 ± 0.97	±	27.53 ± 0.45	±	27.78 ± 0.48
	0.01		0.04		0.04		0.06	

Abbreviation: ED, experimental day.

^aBlinded measurements.

^bCountermeasures.

Statistical methods were used to analyze our results, taking into account probability and the potential for statistically significant results related to chance alone. Statistically significant changes in pH were observed on ED1 (A vs C, $P = .0011$), ED2 (A vs B, $P = .0220$), and ED4 (A vs C, $P = .0280$, and B vs C, $P = .0017$). Although the average electrical conductance of the target water samples tended to be higher than the electrical conductance of each control, those differences were not statistically significant. Nevertheless, with the exception of ED2, these changes were statistically correlated with pH changes, as follows: ED1, $r = .56$, $P = .039$; ED3, $r = .48$, $P = .009$; and ED4, $r = .60$, $P = .001$. On these days, an increase in pH was directly related to an increase in the electrical conductance. As shown in [Table 3](#), countermeasures confirmed blinded measurements and, in the majority of cases, were positively correlated, as follows: ED1, pH, $r = .73$, $P = .003$; ED2, electrical conductance, $r = .48$, $P = .010$; ED3, pH, $r = .45$, $P = .015$, and electrical conductance, $r = .42$, $P = .022$; and ED4, pH, $r = .43$, $P = .019$.

Although we cannot point to a direct cause for the apparent differences, we can hypothetically relate these changes with variables that were also responsive during the experiments, such as the magnetic field strength. Research has shown that electric and magnetic fields have opposite effects over hydrogen-bonded clusters of water. If electromagnetic fields, even extremely low ones, weaken water clustering by reducing the amount of hydrogen bonding and strength, acting as a “disorder-maker” and encouraging reactivity in chemical processes,⁶⁰ then static magnetic fields may seem to strengthen hydrogen bonding, promoting structural coherence.⁶¹⁻⁶³ Even very small magnetic and electromagnetic fields may affect the solubility of gases in water, perturbing the gas-liquid interface and producing reactive oxygen species.⁶⁴ Changes in hydrogen bonding may also affect carbon dioxide hydration resulting in pH changes,⁶⁵ or even promote the gradual decrease of electrical resistivity.⁶⁶

We also used Raman scattering spectroscopy as a tool to assess hypothetical changes in the molecular structure of the water samples. This technique relies on the detection of inelastic scattered light with an origin on the molecular optical vibrations. The frequency and profile of Raman bands are highly specific to both molecular structure

and normal vibrations of the chemical species.⁶⁷ In a standard Raman spectrum, a main double-peak can easily be found in the range of 2900 to 3700 cm^{-1} , known as the OH stretching band, and a smaller, broader band around 1640 cm^{-1} related to the OH bending mode. Usually, the mode around 3200 cm^{-1} is related to strongly hydrogen-bonded water molecules and the mode around 3400 cm^{-1} with loosely bonded ones.⁶⁸ These 2 bands are thought to reflect the dynamic microstructure of water as well as its interactions with solutes, polymers, or biological molecules.⁶⁹ The dynamic equilibrium of water involves changing proportions of different oligomers and polymer species. This cluster structuring process is sensitive to temperature, pressure, composition, magnetic and electric fields, and, as referred to by others, the “subtle energies” of biofield therapies.⁷⁰

As shown in [Figure 6](#), all of the Raman spectra presented the dominant bands related with the vibrational modes known as bending and stretching, and those were coincident with frequencies typically described in the literature. Nevertheless, we noticed different absolute intensities, with a higher expression in the double-peaked OH stretching band. Except on ED2, target water samples presented the highest values. On those days, the intensity followed a specific pattern described as follows, from the highest to the lowest: target water > water around target > control water. Even though the described pattern, discarding the hypothesis of polarization and changes in the concentration, shifts in absolute intensities are often related to source stability and temperature changes of the laser. Thus, to counter these limitations, we decided to evaluate the results taking into consideration the relative intensities between the 2 dominant modes of the OH stretching band.

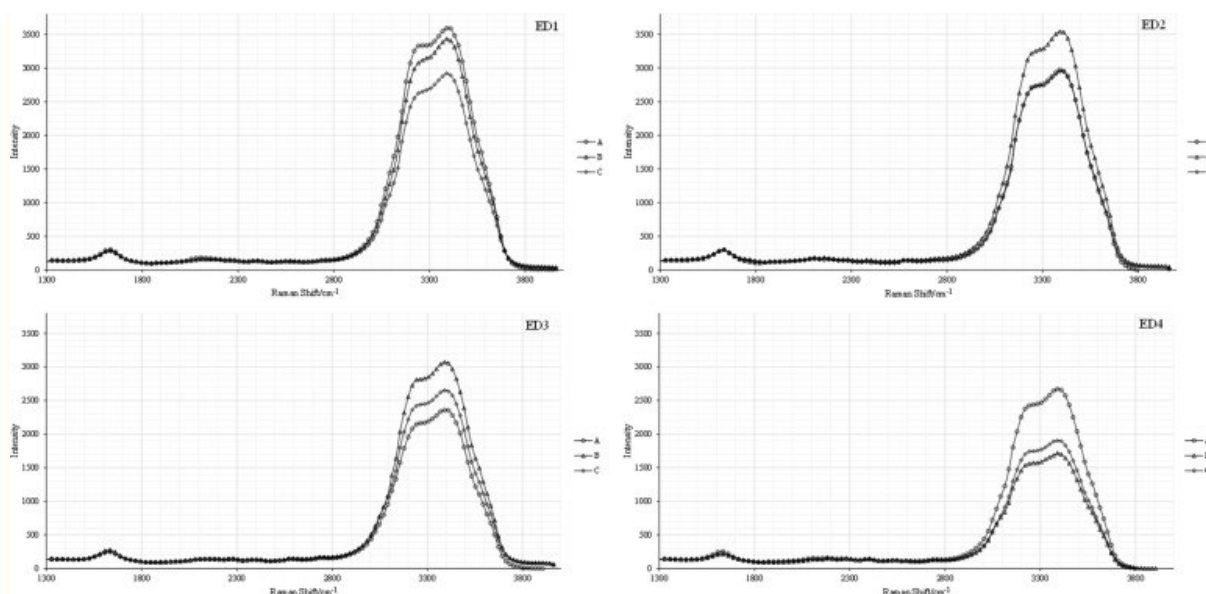
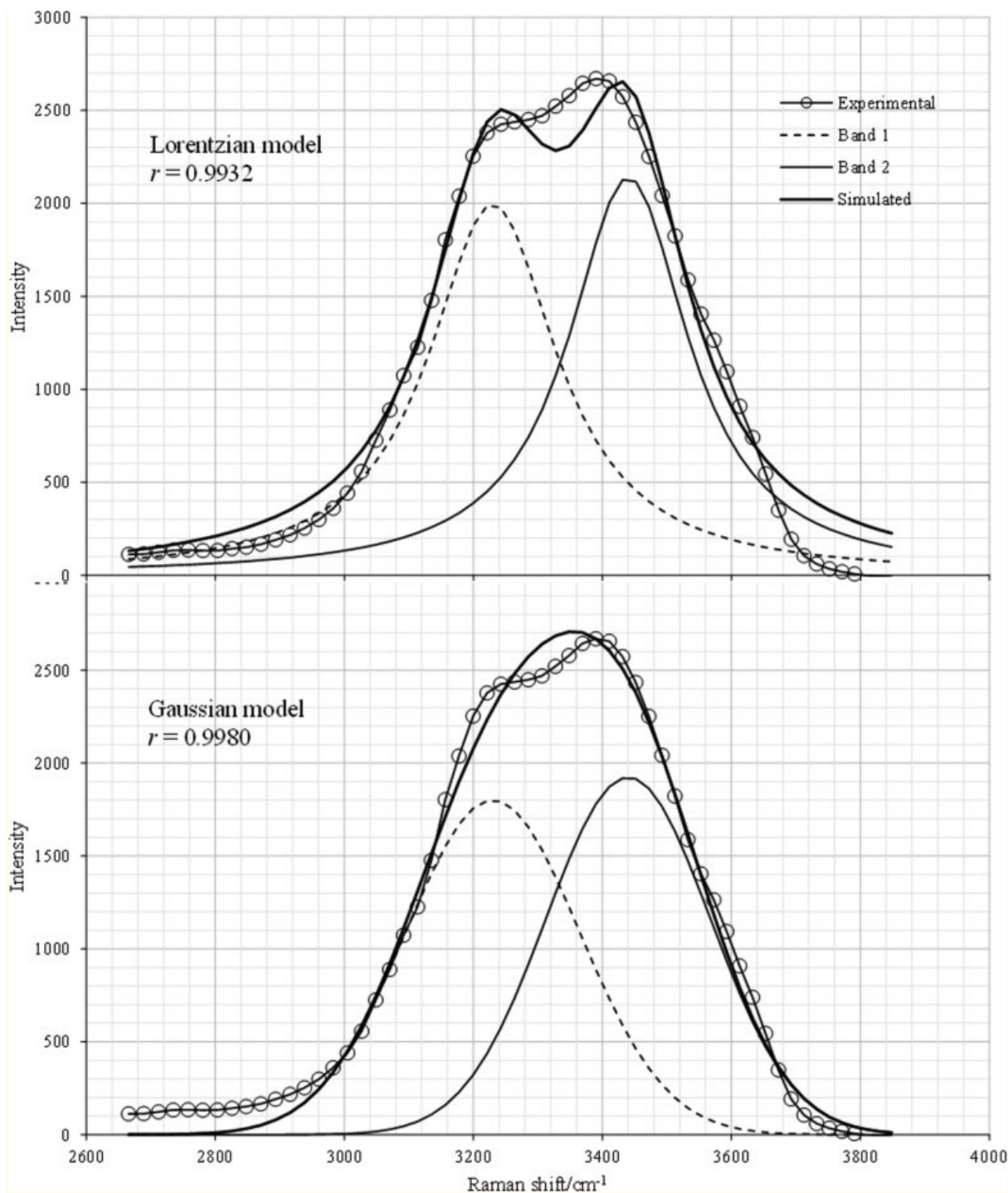


Figure 6.

Raman spectra of the water during the experimental period.

As previously mentioned, we focused our attention on the dominant OH stretching band to evaluate any eventual change that could be related to a shift in the water structure. Peak deconvolution was performed using the Lorentzian and Gaussian functions for 2 peaks centered at 3230 cm^{-1} and 3440 cm^{-1} (an example of this procedure is shown in [Figure 7](#)). The Solver function was used as an optimization method to find the minimum fitting error between the set of experimental data and the proposed model. This procedure allowed us to find the optimal width aspects of both peaks within the OH stretching band.



[Figure 7.](#)

Peak deconvolution of the OH stretching band (target water [A] on the ED4).

Both models provided similar results yielding small fitting errors and high Pearson's correlation coefficients. Bands 1 and 2 for each model and sample were numerically integrated with the trapezoidal rule and the ratios were calculated and compared ([Table 4](#)).

Table 4.

Peak Area Ratios on the Double-Peaked OH Stretching Band (Lorentzian and Gaussian Models).

Peak Area Ratio	Experimental Day	Water Sample					
		A ^a	A ^b	B ^a	B ^b	C ^a	C ^b
$\frac{\int I_{\text{Band1}}}{\int I_{\text{Band2}}}$	ED1	0.93 ± 0.05	0.93 ± 0.05	0.90 ± 0.05	0.89 ± 0.01	0.92 ± 0.00	0.92 ± 0.00
	ED2	0.95 ± 0.24	0.95 ± 0.24	0.89 ± 0.05	0.88 ± 0.06	0.88 ± 0.05	0.88 ± 0.05
	ED3	1.05 ± 0.09	1.05 ± 0.10	0.87 ± 0.04	0.87 ± 0.03	0.95 ± 0.05	0.96 ± 0.05
	ED4	0.99 ± 0.02	0.99 ± 0.03	1.11 ± 0.02	1.14 ± 0.01	1.06 ± 0.02	1.07 ± 0.02

Abbreviation: ED, experimental day.

^aLorentzian model.

^bGaussian model.

Although slight differences in the intensity ratios were observable on ED1, ED2, and ED3, these were not statistically significant.

Nevertheless, on ED4 we found significant differences ($P < .05$) between the control and target water samples (deconvolution with the Lorentzian model) and between the control and both the target and around the target water samples (deconvolution with the Gaussian model).

Conclusions

In science, the results of a study often result in more questions than answers. Our findings are a good example of this statement. Although the phenomenon of intention has been studied by other researchers, the mechanisms behind the most reported outcomes are still unclear or unknown. In our work, we can go no further in the explanation of such interactions than to report that the results of the measurements and the combined analysis of the variables point to changes that were

coincident with specific moments of the experimental period. Given that coincidence does not equate with causality, we can offer no conclusive explanation for the observed changes. Nonetheless, the questions regarding the effects of intention remain relevant and warrant more research.

We can also suppose that this phenomenon, if real, could hypothetically affect neighboring targets. Thus, this raises some ethical issues regarding “distant healing interventions.” Considering a hypothetical scenario in which a person asks for a “distant healing intervention,” we do not know if the effects could affect other persons sharing the same space who are unaware of what is going on.

The time dependence of the eventual effects is also of importance. How long are the changes measurable? Is there any proportional decreasing tendency in the changes as a function of time? Shelf-time experiments should be done to clarify this issue.

Finally, we are aware of the difficulties to reproduce the study, given that it is extremely difficult, if not impossible, to recruit the same 286 practitioners, as well as to ensure the same conditions. Moreover, this high number of participants was based on availability rather than on the knowledge of any proportional effects. Further studies must be conducted to clarify if effects are dependent on the number of practitioners, their levels of expertise, or the duration of the meditation time.

Acknowledgments

We are grateful to all the students, practitioners, and instructors affiliated with Healing Beyond Borders and the Portuguese Association of *Reiki* for their participation in this study. We also thank Liliana Pereira, Department of Chemical Engineering, Faculty of Engineering, University of Porto, for her cooperation.

Footnotes

Author Contributions: LCM conceptualized, designed and managed the study, analyzed the data, and drafted the first manuscript. SCS served as a blinded operator and instrumental analyst. JGA participated in the study design and manuscript preparation. JM advised on data analysis. HJG and FJM are mentors who contributed equally to this work. All authors were active in the editing of this article and approved the final version.

Declaration of Conflicting Interests: The authors declared no potential conflicts of interest with respect to the research, authorship, and/or publication of this article.

Funding: The authors received no financial support for the research, authorship, and/or publication of this article.

ORCID iD: Luís Carlos Matos, MTCM <http://orcid.org/0000-0002-2698-3151>

Sara Cristina Santos, MEng <http://orcid.org/0000-0002-7516-1955>

Ethical Approval: Ethical approval was not required for this study.

References

1. Rubik B. The perennial challenge of anomalies at the frontiers of science. *Br Homoeopathic J*. 1994;83:155–166. [[Google Scholar](#)]
2. Bussard AE. A scientific revolution? *EMBO Rep*. 2005;6:691–694. [[PMC free article](#)] [[PubMed](#)] [[Google Scholar](#)]
3. Oschman JL. Energy and the healing response. *J Bodywork Mov Ther*. 2005;9:3–15. [[Google Scholar](#)]
4. Levin J. Scientists and healers: toward collaborative research partnerships. *Explore (NY)*. 2008;4:302–310. [[PubMed](#)] [[Google Scholar](#)]
5. Chen KW. An analytic review of studies on measuring effects of external Qi in China. *Altern Ther Health Med*. 2004;10:38–51. [[PubMed](#)] [[Google Scholar](#)]
6. Gonella S, Garrino L, Dimonte V. Biofield therapies and cancer-related symptoms: a review. *Clin J Oncol Nurs*. 2014;18:568–576. [[PubMed](#)] [[Google Scholar](#)]
7. Thrane S, Cohen SM. Effect of Reiki therapy on pain and anxiety in adults: an in-depth literature review of randomized trials with effect size calculations. *Pain Manag Nurs*. 2014;15:897–908. [[PMC free article](#)] [[PubMed](#)] [[Google Scholar](#)]

8. Lee MS, Pittler MH, Ernst E. External qigong for pain conditions: a systematic review of randomized clinical trials. *J Pain*. 2007;8:827–831. [[PubMed](#)] [[Google Scholar](#)]
9. Sancier KM, Hu B. Medical applications of qigong and emitted qi on humans, animals, cell cultures, and plants: review of selected scientific research. *Am J Acupunct*. 1991;19:367–377. [[Google Scholar](#)]
10. Hammerschlag R, Marx BL, Aickin M. Nontouch biofield therapy: a systematic review of human randomized controlled trials reporting use of only nonphysical contact treatment. *J Altern Complement Med*. 2014;20:881–892. [[PubMed](#)] [[Google Scholar](#)]
11. Yan X, Shen H, Jiang H, et al. External Qi of Yan Xin Qigong differentially regulates the Akt and extracellular signal-regulated kinase pathways and is cytotoxic to cancer cells but not to normal cells. *Int J Biochem Cell Biol*. 2006;38:2102–2113. [[PubMed](#)] [[Google Scholar](#)]
12. Yan X, Shen H, Jiang H, et al. External Qi of Yan Xin Qigong induces apoptosis and inhibits migration and invasion of estrogen-independent breast cancer cells through suppression of Akt/NF- κ B signaling. *Cell Physiol Biochem*. 2010;25:263–270. [[PubMed](#)] [[Google Scholar](#)]
13. Yan X, Li F, Dozmorov I, et al. External Qi of Yan Xin Qigong induces cell death and gene expression alterations promoting apoptosis and inhibiting proliferation, migration and glucose metabolism in small-cell lung cancer cells. *Mol Cell Biochem*. 2012;363:245–255. [[PMC free article](#)] [[PubMed](#)] [[Google Scholar](#)]
14. Yan X, Shen H, Jiang H, Hu D, Wang J, Wu X. External Qi of Yan Xin Qigong inhibits activation of Akt, Erk1/2 and NF- κ B and induces cell cycle arrest and apoptosis in colorectal cancer cells. *Cell Physiol Biochem*. 2013;31:113–122. [[PubMed](#)] [[Google Scholar](#)]
15. Yan X, Shen H, Zaharia M, et al. Involvement of phosphatidylinositol 3-kinase and insulin-like growth factor-I in YXLST-mediated neuroprotection. *Brain Res*. 2004;1006:198–206. [[PubMed](#)] [[Google Scholar](#)]
16. Hintz KJ, Yount GL, Kadar I, Schwartz G, Hammerschlag R, Lin S. Bioenergy definitions and research guidelines. *Altern Ther Health Med*. 2003;9:A13–A30. [[PubMed](#)] [[Google Scholar](#)]
17. Johnson JA, Stewart JM, Howell MH. *Chinese Medical Qigong Therapy: A Comprehensive Clinical Guide*. Pacific Grove, CA: International Institute of Medical Qigong; 2000. [[Google Scholar](#)]
18. Rubik B. The biofield hypothesis: its biophysical basis and role in medicine. *J Altern Complement Med*. 2002;8:703–717. [[PubMed](#)] [[Google Scholar](#)]

19. Rubik B, Brooks AJ, Schwartz GE. In vitro effect of Reiki treatment on bacterial cultures: role of experimental context and practitioner well-being. *J Altern Complement Med*. 2006;12:7–13. [[PubMed](#)] [[Google Scholar](#)]
20. Rosch PJ. Bioelectromagnetic and subtle energy medicine—the interface between mind and matter. *Ann N Y Acad Sci*. 2009;1172:297–311. [[PubMed](#)] [[Google Scholar](#)]
21. Becker RO, Selden G, Bichell D. *The Body Electric: Electromagnetism and the Foundation of Life*. New York, NY: Quill; 1985. [[Google Scholar](#)]
22. Waechter RL, Sergio L. Manipulation of the electromagnetic spectrum via fields projected from human hands: a Qi energy connection? *Subtle Energies Energy Med J Arch*. 2002;13:233. [[Google Scholar](#)]
23. Joines W, Baumann S, Kim J, Zile J, Simmons C. The measurement and characterization of charge accumulation and electromagnetic emission from bio-energy healers. Paper presented at: the Parapsychological Association Convention; 2004; Vienna, Austria. [[Google Scholar](#)]
24. Waechter RL. *Qi and Bioelectromagnetic Energy*. York, England: York University; 2002. [[Google Scholar](#)]
25. Jobst KA. Science and healing: from bioelectromagnetics to the medicine of light. Implications, phenomena, and deep transformation. *J Altern Complement Med*. 2004;10:1–5. [[PubMed](#)] [[Google Scholar](#)]
26. Moga MM, Bengston WF. Anomalous magnetic field activity during a bioenergy healing experiment. *J Sci Exploration*. 2010;24:397–410. [[Google Scholar](#)]
27. Seto A, Kusaka C, Nakazato S, et al. Detection of extraordinary large bio-magnetic field strength from human hand during external Qi emission. *Acupunct Electrother Res*. 1991;17:75–94. [[PubMed](#)] [[Google Scholar](#)]
28. Hisamitsu T, Seto A, Nakazato S, Yamamoto T, Aung S. Emission of extremely strong magnetic fields from the head and whole body during oriental breathing exercises. *Acupunct Electrother Res*. 1995;21:219–227. [[PubMed](#)] [[Google Scholar](#)]
29. Matthews RE. Harold Burr's biofields measuring the electromagnetics of life. *Subtle Energies Energy Med J Arch*. 2007;18. [[Google Scholar](#)]
30. Schwartz SA, De Mattei RJ, Brame EG, Spottiswoode SJP. Infrared spectra alteration in water proximate to the palms of therapeutic practitioners. *Explore (NY)*. 2015;11:143–155. [[PubMed](#)] [[Google Scholar](#)]
31. Matos L, Goncalves M, Silva A, Mendes J, Machado J, Greten H. Assessment of Qigong-related effects by infrared thermography: a case study. *J Chin Integr Med*. 2012;10:663–666. [[PubMed](#)] [[Google Scholar](#)]

32. Qin Y, Ji H, Chen J, Li H. An applied study of thermography on the acupuncture and qi-gong. Paper presented at: SPIE Proceedings Series. Society of Photo-Optical Instrumentation Engineers; 1997. [[Google Scholar](#)]
33. Oschman JL. *Energy Medicine: The Scientific Basis*. Burlington, VT: Churchill Livingstone, 2000. [[Google Scholar](#)]
34. Oschman JL. *Energy Medicine in Therapeutics and Human Performance*. St Louis, MO: Butterworth-Heinemann; 2003. [[Google Scholar](#)]
35. Engebretson J, Wardell DW. Energy therapies: focus on spirituality. *Explore (NY)*. 2012;8:353–359. [[PubMed](#)] [[Google Scholar](#)]
36. Levin J, Mead L. Bioenergy healing: a theoretical model and case series. *Explore (NY)*. 2008;4:201–209. [[PubMed](#)] [[Google Scholar](#)]
37. Schwartz SA, Dossey L. Nonlocality, intention, and observer effects in healing studies: laying a foundation for the future. *Explore (NY)*. 2010;6:295–307. [[PubMed](#)] [[Google Scholar](#)]
38. Bonilla E. Evidencias sobre el poder de la intención. *Invest Clin*. 2008;49:595–615. [[PubMed](#)] [[Google Scholar](#)]
39. Landon MK. Association of intention with anomalous mind-matter correspondences. *Psychiatr Ann*. 2011;41:e1–e7. [[Google Scholar](#)]
40. Radin D, Hayssen G, Emoto M, Kizu T. Double-blind test of the effects of distant intention on water crystal formation. *Explore (NY)*. 2006;2:408–411. [[PubMed](#)] [[Google Scholar](#)]
41. Radin D, Taft R, Yount G. Effects of healing intention on cultured cells and truly random events. *J Altern Complement Med*. 2004;10:103–112. [[PubMed](#)] [[Google Scholar](#)]
42. Dossey L. Nonlocal mind: a (fairly) brief history of the term. *Explore (NY)*. 2015;11:89–101. [[PubMed](#)] [[Google Scholar](#)]
43. Radin D, Lund N, Emoto M, Kizu T. Effects of distant intention on water crystal formation: a triple-blind replication. *J Sci Exploration*. 2008;22:481–493. [[Google Scholar](#)]
44. Hyland ME. Does a form of “entanglement” between people explain healing? An examination of hypotheses and methodology. *Complement Ther Med*. 2004;12:198–208. [[PubMed](#)] [[Google Scholar](#)]
45. Tiller WA, Dibble WE, Orlando G, Migli A, Raiteri G, Oca J. Toward general experimentation and discovery in conditioned laboratory spaces: part IV. Macroscopic information entanglement between sites ~6000 miles apart. *J Altern Complement Med*. 2005;11:973–976. [[PubMed](#)] [[Google Scholar](#)]

46. Helgeson HL, Peyerl CK, Solheim-Witt M. Quantum physics principles and communication in the acute healthcare setting: a pilot study. *Explore (NY)*. 2016;12:408–415. [[PubMed](#)] [[Google Scholar](#)]
47. Leder D. “Spooky actions at a distance”: physics, psi, and distant healing. *J Altern Complement Med*. 2005;11:923–930. [[PubMed](#)] [[Google Scholar](#)]
48. Rindfleisch JA. Biofield therapies: energy medicine and primary care. *Prim Care*. 2010;37:165–179. [[PubMed](#)] [[Google Scholar](#)]
49. Hammerschlag R, Jain S, Baldwin AL, et al. Biofield research: a roundtable discussion of scientific and methodological issues. *J Altern Complement Med*. 2012;18:1081–1086. [[PubMed](#)] [[Google Scholar](#)]
50. Dibble W, Tiller WA. Electronic device-mediated pH changes in water. *J Sci Exploration*. 1999;13:155–176. [[Google Scholar](#)]
51. Emoto M. Healing with water. *J Altern Complement Med*. 2004;10:19–21. [[PubMed](#)] [[Google Scholar](#)]
52. Emoto M. *The Hidden Messages in Water*. New York, NY: Simon & Schuster; 2011. [[Google Scholar](#)]
53. Yan X, Lu F, Jiang H, et al. Certain physical manifestation and effects of external qi of Yan Xin life science technology. *J Sci Exploration*. 2002;16:381–411. [[Google Scholar](#)]
54. Pajunen GA, Purnell MJ, Dibble WE, Tiller WA. Altering the acid/alkaline balance of water via the use of an intention-host device. *J Altern Complement Med*. 2009;15:963–968. [[PubMed](#)] [[Google Scholar](#)]
55. Tiller WA, Dibble WE. Toward general experimentation and discovery in conditioned laboratory and complementary and alternative medicine spaces: part V. Data on 10 different sites using a robust new type of subtle energy detector. *J Altern Complement Med*. 2007;13:133–150. [[PubMed](#)] [[Google Scholar](#)]
56. Tiller WA, Dibble WE, Nunley R, Shealy CN. Toward general experimentation and discovery in conditioned laboratory spaces: part I. Experimental pH change findings at some remote sites. *J Altern Complement Med*. 2004;10:145–157. [[PubMed](#)] [[Google Scholar](#)]
57. Tiller WA, Dibble WE, Shealy CN, Nunley RN. Toward general experimentation and discovery in conditioned laboratory spaces: part II. pH-change experience at four remote sites, 1 year later. *J Altern Complement Med*. 2004;10:301–306. [[PubMed](#)] [[Google Scholar](#)]
58. Manek NJ. Symmetry states of the physical space: an expanded reference frame for understanding human consciousness. *J Altern Complement Med*. 2011;18:83–92. [[PubMed](#)] [[Google Scholar](#)]

59. Tiller WA, Tiller JE, Dibble WE, Manek R, Manek N. The Buddha relics and evidence of physical space conditioning with unimprinted intention host devices. *J Altern Complement Med*. 2012;18:379–381. [[PubMed](#)] [[Google Scholar](#)]
60. De Ninno A, Castellano AC. On the effect of weak magnetic field on solutions of glutamic acid: the function of water. *J Phys*. 2011;012025. [[Google Scholar](#)]
61. Holysz L, Szczes A, Chibowski E. Effects of a static magnetic field on water and electrolyte solutions. *J Colloid Interface Sci*. 2007;316:996–1002. [[PubMed](#)] [[Google Scholar](#)]
62. Cai R, Yang H, He J, Zhu W. The effects of magnetic fields on water molecular hydrogen bonds. *J Mol Struct*. 2009;938:15–19. [[Google Scholar](#)]
63. Szcześ A, Chibowski E, Hołysz L, Rafalski P. Effects of static magnetic field on water at kinetic condition. *Chem Eng Process*. 2011;50:124–127. [[Google Scholar](#)]
64. Colic M, Morse D. The elusive mechanism of the magnetic “memory” of water. *Colloids Surfaces A*. 1999;154:167–174. [[Google Scholar](#)]
65. Pazur A, Winklhofer M. Magnetic effect on CO₂ solubility in seawater: a possible link between geomagnetic field variations and climate. *Geophys Res Lett*. 2008;35(16). doi:10.1029/2008GL034288. [[Google Scholar](#)]
66. Mohri K, Fukushima M, Matsumoto M. Gradual decrease of electric resistivity in water triggered by Milli-Gauss low frequency pulsed magnetic field. *Trans Magnetism Soc Japan*. 2001;1:22–26. [[Google Scholar](#)]
67. Lopes PC, Moreira JA, Almeida A, et al. Discriminating adenocarcinoma from normal colonic mucosa through deconvolution of Raman spectra. *J Biomed Optics*. 2011;16:127001. [[PubMed](#)] [[Google Scholar](#)]
68. Sun Q. The Raman OH stretching bands of liquid water. *Vibrational Spectrosc*. 2009;51:213–217. [[Google Scholar](#)]
69. Pastorczak M, Kozanecki M, Ulanski J. Raman resonance effect in liquid water. *J Phys Chem A*. 2008;112:10705–10707. [[PubMed](#)] [[Google Scholar](#)]
70. Roy R, Tiller WA, Bell I, Hoover MR. The structure of liquid water; novel insights from materials research; potential relevance to homeopathy. *Mater Res Innov*. 2005;9:98–102. [[Google Scholar](#)]